Doc Number: Beams-doc-4046
Version: 2.0
Category: Note

Activation of Steel and Copper Samples in the Main Injector Collimator Region

Bruce C. Brown
Accelerator Division, Main Injector Department
and
Vernon Cupps*
Radionuclide Analysis Facility, ES&H Section
Fermi National Accelerator Laboratory †
P.O. Box 500
Batavia, Illinois

9 April 2012

*retired
†Operated by Fermi Research Alliance under contract with the U. S. Department of Energy

Contents

1 Introduction **3**

2 Creating and Placing Samples **4**
2.1 Cu and Al Samples . . . 4
2.2 Steel Samples . . . 4
2.3 “Unshielded” and “Shielded” Sampling Locations . . . 5
2.4 Samples placed on June 7 . . . 5
2.5 Samples placed on July 22 . . . 6
2.6 Samples placed on October 5 . . . 6

3 Removing and Measuring Samples **6**
3.1 Samples Removed on July 5 . . . 7
3.2 Samples Removed on July 22 . . . 7
3.3 Samples Removed on July 26 . . . 7
3.4 Samples Removed on August 5 . . . 7
3.5 Samples Removed on November 29 . . . 7
3.6 Samples Removed on December 20 . . . 8

4 Analysis of Activation with Correction for Decay **8**
4.1 Isotope Production . . . 8
4.2 Isotope Production with Decay . . . 9
4.3 Activation Decay Correction Using Detailed History . . . 9
4.3.1 Expression for Intermediate Times . . . 10
4.4 Approximate Corrections for Short or Long Half Life . . . 11
4.5 Graphic Presentation of Corrections . . . 12

5 Results **12**

6 Discussion **18**
6.1 Observation of the Activation of Minor Components . . . 18
6.1.1 Antimony Activation . . . 18
6.1.2 How is ^{59}Fe Produced . . . 19
6.1.3 Apparent fluence from ^{122}Sb, ^{124}Sb and ^{59}Fe . . . 19
6.2 Secular Equilibrium: Do we see long lived isotopes from their daughters? . . . 19

7 Summary and Conclusions **20**

8 Acknowledgments **20**

A Locations for Activation Tag Placement **20**

Abstract

We study the activation of copper tags and steel tags fabricated from the Main Injector laminations by the flux of secondary particles near Main Injector collimator C307. 1.5″ diameter and smaller tags were activated for periods from 3 to 28 days. Two locations are used for the activation, providing different activating spectra and rates. Using a HPGe detector at the Fermilab Radionuclide Analysis Facility (RAF), we measure and analyze the γ-ray spectra to identify the isotopes which have been produced. Normalization to the flux is accomplished by activation studies on Al tags. Detailed decay corrections are aided by pulse-by-pulse loss measurements with the Beam Loss Monitor device LI307. Copper and steel dominates the regions where beam loss activates the Main Injector tunnel so this will help identify the isotopes which dominate the residual radiation. This work is in parallel with a simulation study with MARS and DeTra which informs the measurements. The combination of simulation and measurement will benchmark the simulation system.

1 Introduction

In the Main Injector tunnel, we have localized beam losses which create residual radiation of sufficient levels to require analysis when planning tunnel installation and maintenance activities. In order to better understand the observed residual radiation cool down[1], [2], [3], [4], we have activated samples of copper and of Main Injector lamination steel in secondary fluxes produced by loss of 8 GeV protons. Measurements of the resulting gamma spectrum with a High Purity Germanium (HPGe) detector allow the identification of the isotopes produced.

A series of detailed residual radiation cool down measurements have been carried out near Main Injector Collimator C307[5]. Beams-doc-3717 [4] reports on some of these. A high range Geiger counter for these studies was placed at a forward location ("Unshielded") downstream and above the end of the stainless steel core of C307. Another counter ("Shielded") was placed outside the marble shield on the aisle side above the beam line at approximately the longitudinal center. Images of these locations are provided in Appendix A. Differences in the cool down shapes for residual radiation at these locations were reported[4]. We chose these locations for the activation study since they experience different spectra of secondary particles as well as very different rates.

The Radionuclide Analysis Facility has a shielded box for operation of the HPGe spectrometer. Routine studies using 1.5″ diameter Al disks (tags) employ convenient mounting hardware which is well understood. This study was designed to use this hardware. Initial measurements revealed that multi-week exposures of steel and copper using the same diameter disks resulted in initial activities beyond the rates permitted by the system dead time. These disks were cooled down to provide information on longer half life isotopes. Smaller disks ("Nubs") were fabricated and exposed for shorter times to allow measurement of short half life isotopes.

Since the spatial pattern of beam loss at C307 remains constant, sampling the loss at Beam Loss Monitor (BLM) LI307[6] (integrated for each beam pulse) provides the time history of the activation. In a separate study (Beams-doc-3980[7]) we have measured the secondary hadron flux at the "Shielded" location and related it to the loss recorded by LI307 and to the beam lost on C307 using the Al activation technique. Using the tools developed in [1], we can provide a decay correction for activation of isotopes with half life greater than a couple of hours. We will correct the measured isotope spectra using this information.

Table 1: Nominal Parameters for 1.5″ Activation Analysis Disks

Aluminum Disks				
Density	2.7	gm/cm^3		
Diameter	1.5	in	38.1	mm
Mass	2.31	gm		
Volume	0.86	cm^3		
Thickness	0.08	cm	29.54	mils
Steel Disks				
Density	7.85	gm/cm^3		
Thickness	60	mils	1.52	mm
Diameter	1.5	in	38.1	mm
Volume	1.74	cm^3		
Mass	13.64	gm		
Cu Disks				
Density	8.94	gm/cm^3		
Thickness	44	mils	1.12	mm
Diameter	1.5	in	38.1	mm
Volume	1.27	cm^3		
Mass	11.39	gm		

2 Creating and Placing Samples

2.1 Cu and Al Samples

Activation analysis samples (tags) of pure Al and pure Cu have been secured and labeled by the Radiation Safety Group. Cu samples were obtained from Vernon Cupps at RAF. Al Samples were obtained from both Vernon Cupps and from Gary Lautenschlager. Each tag has a number imprinted (stamped) on its surface. Records are available for the source of each numbered tag. Table 1 gives the nominal properties of the tags. The measured mass of the samples removed on July 22 was 3.058 and 3.048 gm for Al tags and 10.797 gm for the Cu tag. Measurements of the tag masses are reported in the RAF Analysis sheets included in this Beams Document.

2.2 Steel Samples

To provide a definite source of steel for analysis, we selected the lamination steel used for Main Injector dipoles, quadrupoles and sextupoles. We have taken one sextupole lamination (1.52 mm nominal thickness) and cut 1.5″ diameter tags using a water jet cutter. These tags have a nominal weight of 13.64 grams. The tag removed on July 22 has a mass of 13.306 gm. Each sample was then numbered using stamps. For smaller tags, we used one of the steel tags (and one of the Cu tags) and punched smaller circular disks (somewhat deformed from flat by the punch). Sample diameters are shown below for the smaller samples.

In view of the critical magnetic performance requirements on the Main Injector steel, careful chemical analysis was performed on each heat (batch) of the steel. Table 2 provides the reported chemical analysis on one run of the steel. We believe the samples used for this activation study

Table 2: Chemical Analysis of Main Injector Steel Prepared By LTV Steel on 2/22/1995. It reports values from 16 steel slabs from 8 heats in FERMI RUN 6 production for Main Injector. Weight percent is the average for the 16 slabs.

Element	weight percent	Uncertainty on weight %	Std Atomic Weight	molar percent	molar fraction
Fe	Balance		55.845		9.907E-01
C	0.0033	0.0008	12.0107	0.000709738	7.097E-06
Mn	0.5200	0.0100	54.938045	0.5115549	5.116E-03
P	0.0510	0.0030	30.973762	0.028286541	2.829E-04
S	0.0060	0.0010	32.065	0.003445071	3.445E-05
Si	0.3600	0.0100	28.0855	0.181050766	1.811E-03
Al	0.2760	0.0290	26.9815386	0.133349533	1.333E-03
N	0.0023	0.0002	14.0067	0.000576872	5.769E-06
Sb	0.0330	0.0027	121.76	0.071950577	7.195E-04

are typical of the whole production. This report will assume that any chemical variations are small compared with other measurement uncertainties. We note that the analysis form used for each slab listed percent values for several other elements but the quantities were not transferred to the summary. We believe that the amounts shown may have represented limits but in any case those elements are unlikely to be significant.

2.3 "Unshielded" and "Shielded" Sampling Locations

Packets of tags for activation analysis were prepared. For placement at the "Unshielded" (downstream above beam line) location, they sit on the vacuum weldment for the C307 collimator at about 50 milliradian angle with respect to the lost proton interactions (assuming interactions take place at the end of the tapered portion of the vacuum weldment, 14″ from the upstream end). The "Shielded" location is on the aisle side of C307 just above the aluminum support channel for the marble, near the longitudinal center. This puts them 14″ above beam height, 27″ from beam center line and about 18″ downstream of the interaction point. This suggests we are sampling deep in the shower at about 60° from the beam direction. The shielding is provided by the iron and marble which surrounds the stainless steel vacuum box in which the lost 8 GeV beam interacts.

2.4 Samples placed on June 7

Table 3 lists the samples installed on June 7, 2011 to begin activation studies.

Table 3: Activation Samples Installed on June 7, 2011

Sample	C307 Shielded	C307 Unshielded
Al	#5954	#5955
Cu	#1617	#1618
Fe (first)	#001	#002
Fe (second)	#011	#012

These samples were removed at various times as shown below.

2.5 Samples placed on July 22

In response to the discovery that the initial samples were too radioactive for measuring short half life isotopes using the RAF HPGe spectrometer, a new set of samples was prepared. Lower counting rates were achieved by reducing the exposure time and by creating samples with smaller diameters. Cu samples were punched from Cu tag #1623 while Steel samples were punched from tag #018. These tags are identified by the punched diameter. The range of sample sizes was selected to cover the uncertainty in when an additional access would be possible. The reduction in expected activation is indicated in the 'Fraction' column by showing the ratio of area (or weight) for this tag compared with the 1.5″ diameter tags of the same material. Each punched tag has a unique size (shown by the diameter of the punch in inches) to aid identification. Table 4 describes the samples installed on July 22.

Table 4: Activation Samples Installed on July 22, 2011

Sample	C307 Shielded	Fraction	C307 Unshielded	Fraction
Al 1.5″	#6271		#1612	
Cu 1.5″	#1621		#1622	
Steel 1.5″	#003		#004	
Cu	#1623 13/16	0.2934	7/32	0.0214
Cu	#1623 1/2	0.1111	3/16	0.0156
Steel	#018 13/16	0.2934	7/32	0.0214
Steel	#018 1/2	0.1111	3/16	0.0156

2.6 Samples placed on October 5

As results became available from this study, we found that some measurements provided very good agreement between different samples. For example, the Mn-54 activation measurements at unshielded locations agree with a standard deviation of 1.2%. When the agreement of the ratio for "unshielded" *vs.* "shielded" for the 2011 Al tags was not as good as the agreement among the Al tag results in Beams-doc-2980[7], we decided to re-measure the fluence ratio for these locations with additional Al tags. On October 5, the following Al tags were installed:

Table 5: Al Activation Samples Installed on October 5, 2011

C307 Unshielded	C307 Shielded
#6445	#6424
#6434	
#6724	#6185

3 Removing and Measuring Samples

Most of this study was accomplished while the HEP Program required storage of PBar beam in the Recycler Ring (Tevatron and Recycler PBar operation ended on September 30, 2011). Access

to the Main Injector tunnel was restricted since entry required that the 'stash' of antiprotons be used or destroyed. Coordination with the program requirements was achieved with the help of the Run Coordinators.

3.1 Samples Removed on July 5

After 28 days of exposure, we chose to remove one of the steel tags from each sample location. Fe #011 and Fe #012 were removed and delivered to the RAF for analysis. Deadtime considerations limit samples to an observed residual activity of 1 milliRad/hr. Both samples were too hot to measure on July 5. Fe #011 was measured later that week but Fe #012 remains too hot for analysis after 2 months.

Upon delivery to RAF, these tags were assigned to Work Request #: 11-162. Results from MI collimator Tag #011 are available in the report for this work request dated 8/22/2011.

3.2 Samples Removed on July 22

When the activity from the tags removed on July 5 was known, effort began to obtain the tags shown in Table 4. When access was available on July 22, 2011, we removed the remaining sample which had been installed on June 7. These samples were delivered to RAF for analysis and were assigned as Work Request #: 11-179. The results for tags Al#5954, St-#001, Cu#1617 (from "Shielded" location) and Al#5955 (from "Unshielded" location) are in the report for this work request dated 8/31/2011. As expected, the Steel and Cu samples from the "Unshielded" location remain quite hot.

3.3 Samples Removed on July 26

An access was made on July 26 and the samples from the July 22 installation at the "Unshielded" locations were retrieved and delivered to RAF where they were assigned Work Request #: 11-181 (Al#1612) and Work Request #: 11-182 (Cu 7/32 and Steel 7/32). Reports for these two work requests are dated September 16, 2011.

3.4 Samples Removed on August 5

An access was made on August 5 and the samples from the July 22 installation at the "Shielded" locations were retrieved and delivered to RAF where they were assigned Work Request #: 11-196. Results for Al Tag #6271, Steel 13/16 and Cu 13/16 are provided in a report dated September 17, 2011.

3.5 Samples Removed on November 29

On 29 November 2011, removed Al tags #6445, #6434 ("Unshielded") and #6424 ("Shielded") which were installed on October 5. These were delivered to Meka Francis at RAF at 11:20 AM as Work Request #: 11-329. A report on these results prepared by Meka E. Francis is dated December 12, 2011. A file containing these results is included in this document as "AD_MI C-307 Collimator_11-329_gamma.pdf"

3.6 Samples Removed on December 20

On December 20, 2011 at 9:15 AM, Dale White removed the remaining tags which were installed on October 5; Tag #6724 ("Unshielded") and #6185 ("Shielded"). Also Tag #6056 was removed. It had been placed on the aisle side of C307 on 10/12/2007. These tags were measured at RAF under Work Request #: 12-002. A report on these results prepared by Meka E. Francis is dated January 11, 2012.

4 Analysis of Activation with Correction for Decay

The observed isotopes and their approximate abundances will be used to inform our efforts to study the decay of residual radiation on the Main Injector tunnel. For that purpose, the results provided in the RAF standard reports are sufficient. We have additional goals, however. In a parallel efforts, a study of losses in this collimator and of the production of isotopes in these samples is underway using the codes MARS[8][9] and DeTra[10]. For that purpose, the decay corrections during exposure (irradiation) is needed in addition to the cooldown correction applied for the reports which are corrected "back to the time of sampling." The technique to express the results in terms of the hadron fluence (integral of the flux) will be documented here. We will then re-express these results for activation with the simulated uniform flux for 30 days (activation decay correction) and cool down for 2 hours which is the specification we will apply in the simulations. The reader should note that without considering a cool down time, one might expect an unmanageable list of isotopes with short half life. The planning goal for major repair or upgrade activities would involve cool down from a day to a week or more as minimum. However, the monitoring techniques which have been used to develop data on the residual radiation in the Main Injector[1] involve accesses which include some measurements after about 2 hours of cool down.

Our formulas will weight exposure by decay half life and the main result will correct for decay during exposure for any half life. In an attempt to show our results so that the reader compares the measurement with the corrected rate with only modest corrections, we will provide separate relations for long half life and short half life isotopes. We will relate the long half life activation to the total isotope production and the total hadron fluence (integrated flux) with a correction for decay during irradiation. For short half life isotopes, the preferred relation compares the activation or isotope production rate with the hadron flux (rate).

4.1 Isotope Production

In a beam of particles, nuclear interactions produce new isotopes. The number of new nuclei is proportional to the fluence, Φ, measured in particles per unit area (particles-cm^{-2}). In a material with n_T target atoms per unit volume, an interaction with cross section σ_I will produce n_I atoms per unit volume of isotope I

$$n_I = \Phi n_T \sigma_I. \tag{1}$$

Given a decay constant of τ_I or a half life of $t_{1/2}$, the activity, S_A (Bq per cm^3), produced by n_I atoms per cm^3

$$S_A = \frac{n_I}{\tau_I} = \frac{n_I \ln 2}{t_{1/2}} = \frac{\Phi n_T \sigma_I \ln 2}{t_{1/2}} \tag{2}$$

We will want the specific activity per gram of target material, $S_A = S/\rho_T$ (Bq per gram).

$$S_A(Bq/gm) = \frac{n_I \ln 2}{\rho_T\, t_{1/2}} = \frac{\Phi n_T \sigma_I \ln 2}{\rho_T\, t_{1/2}} \tag{3}$$

Substituting for n_T with $\rho_T N_A / A_T$ we have

$$S_A(Bq/gm) = \frac{\Phi N_A \sigma_I}{A_T\, \tau_I} = \frac{\Phi N_A \sigma_I \ln 2}{A_T\, t_{1/2}} \tag{4}$$

$$S_A(pCi/gm) = \frac{\Phi N_A \sigma_I \ln 2}{A_T\, t_{1/2}\, 3.7 \times 10^{-2}} \tag{5}$$

4.2 Isotope Production with Decay

Let us derive the standard activation formula [following Barbier[11], see page 15, Eq 3.9] which relates the activation to the flux of particles which produces the radioactive isotope. For a flux, $\frac{d\Phi(t)}{dt}$

$$n_I(t) = n_T \sigma \int_0^{t_i} \frac{d\Phi(t)}{dt} e^{-(t_i-\tau)/\tau_I} d\tau \tag{6}$$

For a constant flux,

$$n_I(t) = n_T \sigma \frac{d\Phi}{dt} \tau_I (1 - e^{-t_i/\tau_I}) \tag{7}$$

After a cooling time, t_c, the number of atoms will have decayed to

$$n_I(t_c) = n_T \sigma_I \frac{d\Phi}{dt} \tau_I (1 - e^{-t_i/\tau_I}) e^{-t_c/\tau_I} \tag{8}$$

in agreement with Eq 3.9 of Barbier. Equation 5 describes the activity for each isotope produced by the fluence Φ before considering the decay losses during irradiation and during cooldown. Dividing Eq. 8 by τ_I, we have the activation,

$$S_A(t_c)(Bq/cm^3) = \frac{n_I(t_c)}{\tau_I} \tag{9}$$

We again convert to activity per gm by using molar quantities to obtain the standard activation equation.

$$S_A(t_c)(Bq/gm) = \frac{N_A \sigma_I}{A_T} \frac{d\Phi}{dt} (1 - e^{-t_i/\tau_I}) e^{-t_c/\tau_I} \tag{10}$$

Correction for decay after exposure is done in the RAF analysis so for analysis in this report we will set $t_c = 0$. We observe that for short half life isotopes, $t_i \gg \tau_I$, the activation is proportional to the flux. We will show that for $\tau_I \gg t_i$, the activation is proportional to the fluence.

4.3 Activation Decay Correction Using Detailed History

We have details of the activation time history using the BLM record (see [1]). We use the fluence from the activation of Al tags. To correct the measured activities for decay during irradiation, we apply the half life weighted BLM histories as follows. We sum loss per pulse (per Main Injector cycle) using

$$LI_j = \sum_{t=t_j}^{t_j+T_s} LI(t) \tag{11}$$

where the sum interval T_s used is 10 minutes for each quanta LI_j. To account for decays, we will weight these to provide an exponentially weighted sum but express the life time using the half life

$$LW(I,T_M) = \sum_j LI_j \frac{\ln 2}{t_{1/2}} 2^{-(T_M-T_j)/t_{1/2}} \tag{12}$$

where T_M is the radiation measurement time, T_j is the quanta time and $t_{1/2}$ is the half life for isotope I. With times in seconds, LW is in units of Rads/sec. For times which are long compared with $t_{1/2}$, LW approaches the average loss rate in Rads/sec. The sum loss without weighting

$$L(I,T_M) = \sum_j LI_j \frac{\ln 2}{t_{1/2}} \tag{13}$$

now allows the correction we need. We can provide the fluence or activity (corrected for decays) by

$$\frac{\Phi}{\Phi_{uncorr}} = \frac{S_A}{S_{A(uncorr)}} = \frac{L(I,T_M)}{LW(I,T_M)} \tag{14}$$

For our case of nearly uniform irradiation, this will produce a similar result as will Equation 20. For short half life isotopes, this correction will not be large and comparison of corrected and uncorrected results will be apparent.

For the long half life isotopes, where the integral flux is simply related to the observed activation, we will remove the normalization to the half life and define "un-normalized" sums as follows:

$$LWu(I,T_M) = LW(I,T_M)\frac{t_{1/2}}{\ln 2} = L(I,T_M)\tau_I \tag{15}$$

$$Lu(I,T_M) = L(I,T_M)\frac{t_{1/2}}{\ln 2} = L(I,T_M)\tau_I \tag{16}$$

Note that $LWu(I,T_M)$ and $Lu(I,T_M)$ will have units of Rads rather than Rads/sec. Most of the results for Aluminum tag activation in Beams-doc-3980[7] employed $LWu(I,T_M)$ and $Lu(I,T_M)$ for normalization to the BLM record. Look there for a study of these corrections for Al Tag activation.

4.3.1 Expression for Intermediate Times

Since we will use a spreadsheet for some of the calculations for half life weighted loss, we will want to be able to select the beginning time for the exposure of interest from a table of losses beginning at an earlier time. Let us call T_s the time for starting the exposure of interest.

$$LW(I,T_M) = \sum_j LI_j \frac{\ln 2}{t_{1/2}} 2^{-(T_M-T_j)/t_{1/2}} = \sum_j^{j_s} LI_j \frac{\ln 2}{t_{1/2}} 2^{-(T_s-T_j)/t_{1/2}} 2^{-(T_M-T_s)/t_{1/2}} + \sum_{j=j_s}^{j_M} LI_j \frac{\ln 2}{t_{1/2}} 2^{-(T_M-T_j)/t_{1/2}} \tag{17}$$

$$LW(I,T_M) = LW(I,T_s)2^{-(T_M-T_s)/t_{1/2}} + \sum_{j=j_s}^{j_M} LI_j \frac{\ln 2}{t_{1/2}} 2^{-(T_M-T_j)/t_{1/2}} \tag{18}$$

$$LW(I,T_M-T_s) = LW(I,T_M) - LW(I,T_s)2^{-(T_M-T_s)/t_{1/2}} \tag{19}$$

4.4 Approximate Corrections for Short or Long Half Life

With the assumption of uniform exposure, we can find an expression equivalent to the formula in Eq. 14 by dividing Eq. 10 by Eq. 4 where we note that for uniform exposure, $\Phi = t_i \frac{d\Phi}{dt}$. Taking $t_c = 0$,

$$\frac{S_A(t_i)}{S_A(produced)} = \frac{\tau_I}{t_i}(1 - e^{-t_i/\tau_I}) \tag{20}$$

For $\tau_I \gg t_i$, (long half lives) this reduces to

$$\frac{S_A(t_i)}{S_A(produced)} \sim (1 - t_i/2\tau_I + \cdots) \tag{21}$$

and we find a simple and potentially small correction to the produced activation.

For short half life isotopes, with $t_i \sim \tau_I$ or even larger, the decay will match the production and this ratio in Eq.20 will get very small. To see the effect of corrections for decay during activation with these isotopes, it is more useful to just examine Eq. 10 and note that the activity will approach a value proportional to flux with a correction which falls as e^{-t_i/τ_I}. We can get the desired result for all cases by manipulating Eq. 14,

$$S_A = S_A(meas)\frac{L(I,T_M)}{LW(I,T_M)} \tag{22}$$

$$\frac{S_A}{L(I,T_M)} = \frac{S_A(meas)}{LW(I,T_M)}. \tag{23}$$

where the ratio on the left hand side expresses that the total activity produced is related to the total fluence while the right hand side expresses the fact that the observed activity is proportional to the flux.

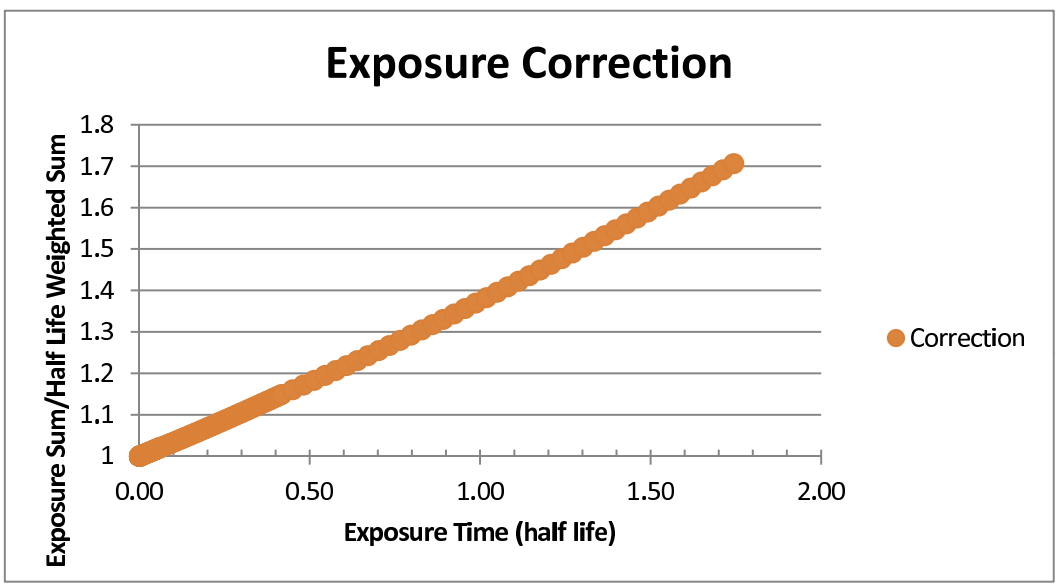

Figure 1: For long half life isotopes, the observed activation requires only the small correction given by $\frac{L(I,T_M)}{LW(I,T_M)}$ which is what is shown in this figure.

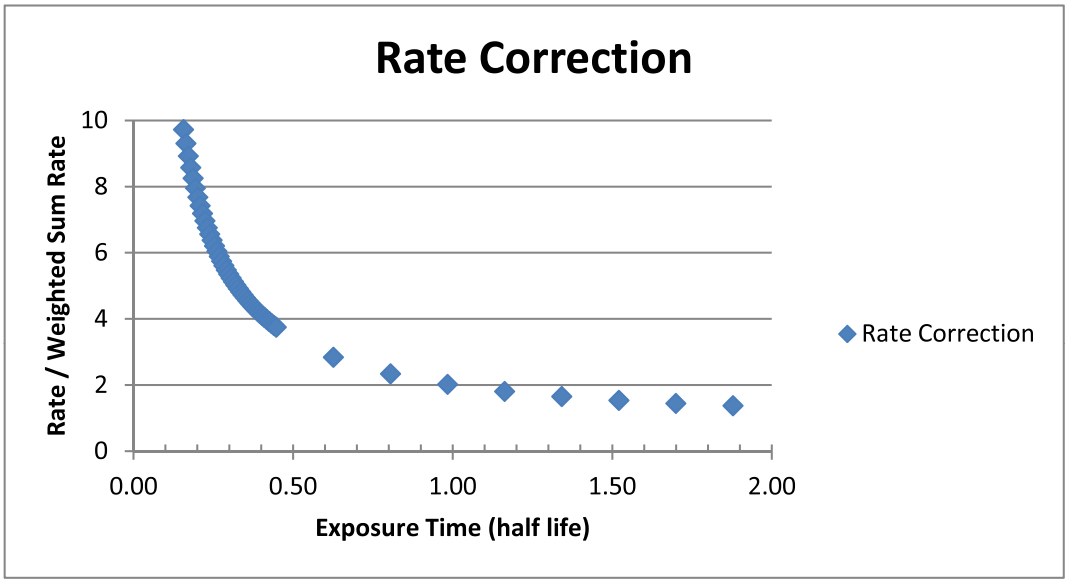

Figure 2: For short half life isotopes, the observed activation is nearly that provided by a constant production rate. A correction given by $\frac{LW(I,T_M)}{L(I,T_M)}$ as shown in this figure provides the needed result.

4.5 Graphic Presentation of Corrections

To support the observations above about the size of corrections, we illustrate the two cases in Figures 1 and 2. We will show that most of these activation measurements show consistency only at the 2% to 10% range so well measured corrections of 50% should present no limitation for our measurement precision. For the short half life measurements, the corrections become small after one lifetime. The correction formulas for the two cases are simply the inverse of each other. The results below correct with this scheme and should provide reliable answers for all measurements.

5 Results

To present results which allow one to compare various exposures but are based as much as possible on a limited set of corrections, we will report results using $S_A(meas)/LW(I,T_M)$, *i. e.* we will use the use the activities as reported by RAF analysis which corrects for decay after the exposure while taking the ratio to the LI307 ten minute weighted sums (using the known isotope half life) which will correct for decay during exposure. In Tables 6 and 8, we provide the results for individual tags. Table 7 shows the average of the available steel results for the shielded location and compares the ratio of individual results to that mean. The standard deviation for this ratio is 1.2% for Mn-54 but it ranges from 2% to 10% for most other isotopes. Considering all measured ratios to the mean we have a standard deviation of 26%. For the ratio of unshielded to shielded location activation for steel, the ratio is based on the mean of the results for three tags when that is available. For copper we give the ratio for one tag in each location. We show the copper results and ratios in Table 8.

Note that by using the activation weighted by the BLM measurements, we have the most direct comparison among samples. This also provides the most direct ratios of steel to copper and of unshielded to shielded locations. The reader is encouraged to use these ratios in any of many combinations so comparisons will not be made here. These calculated results and other information

is available as a file in the document database entry as SteelActData.xls and CopperActData.xls.

Measurements expressed as S_A/LW compare the activation in the sample to the average loss in the nearby loss monitor in Rads/second. For long half life isotopes, this activation will not typically be reached in the period between long facility shutdowns. In comparing with MARS calculations, we will need to make the cool down corrections to match the MARS simulation conditions.

In preparation for comparison with MARS calculations, we have applied Equation 20 and the decay correction (as in Equation 10) to produce a table of corrections for each observed isotope. The results of this calculation are in worksheet IsotopeDecayCorr of spreadsheet SteelActData and are presented here in Table 9.

Table 6: Steel Sample Results Normalized to Weighted Sums for LI307

Sample	Half Life days	St #011 Shielded	St #001 Shielded	St 13/16 Shielded	St 7/32 Unsh
		S_A/LW (pCi/gm)/(Rad/sec)			
Ar-42/K-42	12020.4				1.6715E+09
Br-76	0.675			1.9640E+04	
Co-60	1925.8	1.5009E+05	1.2689E+05		
Cr-48	0.8983				2.2483E+05
Cr-51	27.7	2.7771E+05	2.9005E+05	2.8482E+05	2.8584E+07
Fe-52	0.34479			1.2668E+03	2.5584E+05
Fe-59	44.5	3.1089E+05	3.2703E+05	3.4429E+05	
K-43	0.9292				3.2431E+05
Mn-52	5.591	7.8784E+04	8.6647E+04	7.1730E+04	8.1052E+06
Mn-54	312.2	6.4859E+05	6.3301E+05	6.3673E+05	6.3507E+07
Mn-56	0.1074			6.7716E+06	3.0780E+07
Na-24	0.62329			4.1047E+03	2.4362E+05
Sb-122	2.7	5.5215E+05	5.8856E+05	5.1685E+05	1.0579E+06
Sb-124	60.2	2.8151E+05	2.6412E+05	6.0953E+04	
Sc-44m	2.44	7.7390E+03	5.2634E+03	3.1531E+03	1.4043E+06
Sc-46	83.83	1.5582E+04	1.8122E+04		3.6293E+06
Sc-47	3.341	8.4731E+03	1.2754E+04	9.8253E+03	1.3634E+06
Sc-48	1.82	1.6546E+03		2.4429E+03	2.2196E+05
Ti-44/Sc-44	17275.85	4.6064E+06		2.5732E+07	1.2218E+10
V-48	15.98	5.0970E+04	4.8654E+04	4.2489E+04	7.0597E+06
Sc-44	0.165417	6.5241E+03		1.4236E+04	2.8871E+06
K-42	0.515				3.9625E+05

Instead of normalizing our activation to BLM response or even beam loss, we can use Al activation as a measure of the hadron fluence. Little correction for decay will be required since the exposures (in days) and maximum corrections (in parentheses) for 2011 are 27.94 (Steel only) , 44.76 (3.3%), 3.92 (0.29%), 13.87 (1.02%), 55.01 (4.09%) and 75.93 (5.69%) but we will use the decay corrected values anyway. Activation results are from the reports for Work Requests # 11-179, Work Request # 11-181, Work Request #: 11-196, Work Request #11-329 and Work Request #: 12-002. Table 10 presents measured activations. The fluence in the 5th column has not been corrected for decay (but that is small).

To examine the repeatability of our measurements, we compare activity divided by the cor-

Table 7: Ratios for Steel Samples

		S_A/LW	Shielded			Unshielded
Sample	Half Life days	Average Shielded	St #011 /average	St #001 /average	St 13/16 /average	St 7/32 /average
Ar-42/K-42	12020.4					
Br-76	0.675	1.9640E+04				
Co-60	1925.8	1.3849E+05	1.084	0.916		
Cr-48	0.8983					
Cr-51	27.7	2.8419E+05	0.977	1.021	1.002	100.578
Fe-52	0.34479	1.2668E+03				201.957
Fe-59	44.5	3.2740E+05	0.950	0.999	1.052	
K-43	0.9292					
Mn-52	5.591	7.9054E+04	0.997	1.096	0.907	102.527
Mn-54	312.2	6.3944E+05	1.014	0.990	0.996	99.316
Mn-56	0.1074	6.7716E+06				4.545
Na-24	0.623	4.1047E+03				59.352
Sb-122	2.7	5.5252E+05	0.999	1.065	0.935	1.915
Sb-124	60.2	2.0219E+05	1.392	1.306	0.301	
Sc-44m	2.44	5.3852E+03	1.437	0.977	0.586	260.775
Sc-46	83.83	1.6852E+04	0.925	1.075		215.362
Sc-47	3.341	1.0351E+04	0.819	1.232	0.949	131.716
Sc-48	1.82	2.0488E+03	0.808		1.192	108.340
Ti-44/Sc-44	17275.85	1.5169E+07	0.304		1.696	805.470
V-48	15.98	4.7371E+04	1.076	1.027	0.897	149.030
Sc-44	0.1654	1.0380E+04	0.629		1.371	278.141
K-42	0.515					

Table 8: Copper Sample Results and Ratios Normalized to Weighted Sums for LI307

Sample	Half Life days	Cu #1617 Shielded	Cu 13/16 Shielded	Cu 7/32 Unshielded	Cu 7/32 / Cu#1617
		S_A/LW (pCi/gm)/(Rad/sec)			
Ag-110m	249.95	2.0437E+05			
Au-198	2.69517	9.8701E+03			
Co-55	0.730417			3.8852E+05	
Co-56	77.233	2.2946E+04		4.6425E+06	2.0232E+02
Co-57	271.74	1.2002E+05		1.3501E+07	1.1249E+02
Co-58	70.86	1.9304E+05	4.8881E+05	2.1993E+07	1.1393E+02
Co-60	1925.8	1.3154E+05			
Cr-51	27.7	2.0319E+04			
Cu-61	0.1389			1.9978E+07	
Cu-64	0.52917	2.6090E+08	6.2781E+08	4.9439E+08	1.8949E+00
Fe-59	44.5	1.3874E+04			
K-43	0.9292			2.0923E+05	
Mn-52	5.591	8.6647E+03	1.5780E+04	1.6017E+06	1.8486E+02
Mn-54	312.2	4.8838E+04			
Mn-56	0.1074			2.7428E+06	
Na-24	0.62329			6.1163E+04	
Ni-57	1.483			3.7067E+05	
Sc-44m	2.44			3.7668E+05	
Sc-47	3.341			2.2177E+05	
Sc-48	1.82			1.3058E+05	
Se-75	119.779	6.8359E+03			
Ti-44/Sc-44	17275.85			2.3386E+09	
V-48	15.98	5.3139E+03		8.2708E+05	1.5564E+02
Sc-44	0.165417			5.5261E+05	

Table 9: Correction of Decay during 30 Day exposure and 2 hr cooldown.

Isotope	Half Life	Exposure	Cooldown	Product
	Days	Correction	Correction	
Ag-110m	249.95	0.9595328	0.999768931	0.959311082
Ar-42	12020.4	0.999135535	0.999995195	0.999130734
Br-76	0.675	0.032460638	0.917985461	0.029798394
Co-55	0.730417	0.035125633	0.92396488	0.032454851
Co-56	77.233	0.876689278	0.999252383	0.87603385
Co-57	271.74	0.962695976	0.999787458	0.962491363
Co-58	70.86	0.866629946	0.999185172	0.865923792
Co-60	1925.8	0.994620477	0.999970007	0.994590644
Cr-48	0.89833	0.043200701	0.937724233	0.040510345
Cr-51	27.7	0.703295292	0.997916892	0.701830253
Cu-61	0.1389	0.006679678	0.659775905	0.004407091
Cu-64	0.52917	0.025447698	0.896590226	0.022816157
Fe-52	0.344791	0.016580974	0.845752919	0.014023407
Fe-59	44.5	0.798865026	0.998702814	0.79782875
K-43	0.9292	0.044685074	0.939729288	0.041991873
Mn-52	5.591	0.262349687	0.98972189	0.259653228
Mn-54	312.2	0.967424209	0.999815	0.967245236
Mn-56	0.1074	0.005164848	0.58401787	0.003016364
Na-24	0.62329	0.029973913	0.911491347	0.027320962
Ni-57	1.483	0.071317167	0.961799177	0.068592792
Sb-122	2.7	0.129783854	0.978833785	0.127036821
Sb-124	60.2	0.845569846	0.999040954	0.844758906
Sc-44m	2.44	0.117315848	0.976604949	0.114571238
Sc-46	83.83	0.885622219	0.999311197	0.8850122
Sc-47	3.341	0.160349808	0.982859681	0.157601361
Sc-48	1.82	0.087522544	0.96876084	0.084788413
Se-75	119.779	0.918009285	0.999517876	0.91756669
Ti-44	17275.85	0.999398407	0.999996656	0.999395065
V-48	15.98	0.55930893	0.996391865	0.557290868
Na-22	950.610	0.989141912	0.999939238	0.989081811
Sc-44	0.165417	0.00795486	0.705257331	0.005610223
K-42	0.515	0.024766265	0.893901456	0.0221386
Na-22	950.6101	0.989141912	0.999939238	0.989081811

Table 10: Activation and Fluence for Al Tags

Tag	Location	Removal	Activation(pCi/g)	Fluence(hadrons/cm^2)
Al#5955	Unshielded	7/22/2011 9:20 AM	60,800 $\pm$ 9,200	1.1824E+15
Al#1612	Unshielded	7/26/2011 9:37 AM	355 $\pm$ 55	6.904E+12
Al#6434	Unshielded	11/29/2011 11:20 AM	21,300 $\pm$3,200	4.143E+14
Al#6445	Unshielded	11/29/2011 11:20 AM	25,100 $\pm$3,800	4.882E+14
Al#6724	Unshielded	12/20/2011 09:15 AM	32,200 $\pm$4,900	6.262E+14
Al#5954	Shielded	7/22/2011 9:20 AM	45.8 $\pm$ 11.8	8.907E+11
Al#6271	Shielded	8/05/2011 11:30 AM	13.9 $\pm$ 2.9	2.703E+11
Al#6424	Shielded	11/29/2011 11:20 AM	54.1 $\pm$ 9.8	1.052E+12
Al#6185	Shielded	12/20/2011 09:15 AM	80.5 $\pm$ 14.0	1.566E+12
Al#6325	Shielded	10/08/2008	339 $\pm$ 56	6.593E+12
Al#6168	Shielded	08/26/2009	1020 $\pm$ 160	1.984E+13
Al#6559	Shielded	08/12/2010	1,740$\pm$ 260	3.384E+13
Al#6056	Shielded	12/20/2011	1,660$\pm$ 250	3.228E+13

Table 11: Normalized Results for Al Tags

Tag	Location	S_A/LW	Ratio to	Fluence/LW
		(pCi/g)/(Rad/sec)	average	(hadrons/cm^2/(Rad/sec))
Al#5955	Unshielded	1.7639E+08	2.219	3.430E+18
Al#1612	Unshielded	3.1117E+07	0.392	6.052E+17
Al#6434	Unshielded	5.8714E+07	0.739	1.142E+18
Al#6445	Unshielded	6.9189E+07	0.871	1.346E+18
Al#6724	Unshielded	6.1968E+07	0.780	1.205E+18
Al#5954	Shielded	1.3287E+05	0.896	2.584E+15
Al#6271	Shielded	1.8984E+05	1.280	3.692E+15
Al#6424	Shielded	1.4913E+05	1.006	2.900E+15
Al#6185	Shielded	1.5492E+05	1.045	3.013E+15
Al#6325	Shielded	1.1762E+05	0.793	2.288E+15
Al#6168	Shielded	1.3756E+05	0.928	2.675E+15
Al#6559	Shielded	1.5974E+05	1.077	3.107E+15
Al#6056	Shielded	1.4445E+05	0.974	2.809E+15

Table 12: Averaged Results for Al Tags

Tags to average	#	S_A/LW	RMS/Mean	Fluence/LW
		(pCi/g)/(Rad/sec)		(hadrons/cm^2/(Rad/sec))
Unshielded	5	7.9475E+07	0.705	1.546E+18
Unshielded(Exclude #5955)	4	5.5247E+07	0.302	1.074E+18
Unshielded(Exclude #5955,#1612)	3	6.3291E+07	0.085	1.231E+18
Shielded	8	1.4827E+05	0.144	2.884E+15
Shielded (Inst 2011)	4	1.5669E+05	0.153	3.0473E+15
Shielded (Inst 2007)	4	1.3984E+05	0.125	2.7198E+15

rected BLM rate. Table 11 shows the results for each tag and also converts these results to a hadron fluence per BLM rate. The "Ratio to average" column in this table compares each tags to all other tags at the similar location. Table 12 shows various averages of these data.

Since some sets of results are in better agreement, we compare both the complete set and various subsets to gain an understanding of the internal agreement of our data. The Al tags placed in 2007 were about 15 cm further upstream than the other "shielded" tags. Their average activation is about 12% (about 1 sigma) lower than the "shielded" tags placed in 2011. We will consider results for these sets separately and together.

The Al tag results from tags placed in June and July showed less consistency than was observed in the larger set of Al tag data examined in Beams-doc-3980[7]. As a result, we remeasured Al activation with the tags placed on October 5. The ratio for #5955/#5954 of 1328 is strikingly different than the ratio of #1612/#6271 of 164. Re-measurement of #5955 confirmed the measured activation. An additional measurement was needed. The results for the tags placed on October 5 were in good agreement and provide a ratio of hadron fluences for "unshielded"/"shielded" of 416. Lacking evidence that conditions changes from July to October, we prefer this measurement to the one obtained while the Cu and Steel samples were being irradiated.

6 Discussion

A few of the measurement results are particularly interesting. We had recognized the possibility of producing various isotopes which have half live values between 15 and 80 days. We believed that the limited residual radiation data we are able to obtain would not be appropriate for identifying these isotopes by separating their contribution to cool down measurements. We have added the half life values for ^{51}Cr and ^{59}Fe to the array of possibilities we consider for fitting residual radiation to BLM history[1]. Several other items deserve separate consideration.

6.1 Observation of the Activation of Minor Components

The existence of large differences in cross section creates the possibility of seeing the activation and identification of minor components of the materials under study.

6.1.1 Antimony Activation

Our first surprise when examining the activation of steel sample #011 was the appearance residual radiation from ^{122}Sb and ^{124}Sb. As noted in Table 2, Sb is only 0.0330% by weight. By taking

the activation measurements and half life values in the measurements for Sample #011 or #001, we can see an interesting range for the effect of Sb on the observed residual radiation near activated Main Injector steel. After two days, the contribution is 25 - 50% depending on the activation history. After 60 to 90 days cool down, these results imply that the Sb isotopes contribute about 25% of the residual radiation. After some consideration, we suspect that neutron capture is responsible for much of this activation. We note that the molar fraction of ^{121}Sb is 0.5721 and for ^{123}Sb the molar fraction is 0.4279. Fortunately the high loss points in the Main Injector frequently do not have Main Injector laminations at the loss locations, since the focusing in regular cells is by older Main Ring Quadrupoles and Main Injector Lambertsons used different steel. The Bar-coded monitoring points include many Main Injector trim dipoles (IDH or IDV) which are also made with a different silicon steel material. Attention to this issue is needed when examining the MARS/DeTra simulation for sample activation.

Was this antimony an impurity on an additive? We consulted with a consultant on steel for the Main Injector Project[1] who provided us, as an answer, with a reference entitled "Influence of Antimony on the Texture and Properties of 2% Si, 0.3% Al Steel for Non-Oriented Sheet"[12].

6.1.2 How is ^{59}Fe Produced

We notice that the measured spectra include significant production of ^{59}Fe in the steel samples. Looking at the materials in the steel, we notice that pure iron includes 4 isotopes. ^{58}Fe is only 0.00282 mole fraction. We might not be surprised if the routine MARS calculation fails to sample the reaction for neutron capture on ^{58}Fe which will produce ^{59}Fe due to limited statistics. We expect to examine this carefully.

6.1.3 Apparent fluence from ^{122}Sb, ^{124}Sb and ^{59}Fe

Using known cross sections for n,γ reactions, a calculation of the required flux to produce these isotopes with that reaction was carried out (see worksheet LowENeutronFlux in SteelActData.xls). The implied fluence from the various reactions differs by a factor of 10. We compare the apparent flux to the flux above 30 MeV obtained by Al activation and find that this flux is comparable but smaller. Since these reactions are exothermic and therefore without threshold, the effects of the flux of low energy neutrons at these sample locations is not understood. It is apparent that the spectrum to which the samples were exposed is significant in understanding the details of this activation process. As is apparent from the results shown above, the ^{124}Sb activation is not well determined in these studies.

6.2 Secular Equilibrium: Do we see long lived isotopes from their daughters?

We have examples of isotope pairs which can occur with production of a long lived isotope in combination with a short lived daughter. Once the originally produced daughters decay, one achieves secular equilibrium between the long lived and short lived components. We identify the decay of the short lived isotope and then must have additional data to learn about what is produced. Table 13 shows the examples in these measurements. We identify these pairs from the decays of K-42 and Sc-44.

In the copper samples, we only see Sc-44 in the "Unshielded" sample (Cu-7/32) which was counted quickly. If we assume we produced Sc-44 directly, it appears at about the same rate as

[1] We thank Dr E.W. Collings, Department of Materials Science and Engineering, Laboratories for Applied Superconductivity and Magnetism (LASM), The Ohio State University for providing us with this information.

Table 13: Secular Equilibrium Candidates

Ar-42/K-42				
Ar-42	12020.4	days	32.9	years
K-42	0.515	days	12.360	hours
Ti-44/Sc-44				
Ti-44	17275.85	days	47.3	years
Sc-44	0.1654	days	3.97	hours

Sc-44m. In the steel samples, we see both K-42 and Sc-44 in the "Unshielded" sample (Steel-7/32) which was counted quickly. We also see Sc-44 in the "Shielded" sample (Steel-13/16) which was counted quickly and also in Steel#011. Since we have other samples which should have adequate sensitivity but were measured after more delay, most or all of the activity must be due to the production of the short lived isotopes. We conclude that one should ignore the lines in Tables 6, 7 and 8 for Ar-42/K-42 and Ti-44/Sc-44, using instead the lines for K-42 and Sc-44.

7 Summary and Conclusions

The activation of steel and copper in the secondary flux produced by 8 GeV protons which strike a Fermilab Main Injector collimator has been measured. A "shielded" location which sees a heavily attenuated, large angle flux is compared to an "unshielded" location which sees a heavily attenuated but very forward flux. For most of the isotopes which are produced, the ratio is greater than 100. For the copper samples, the production of ^{64}Cu dominates in the "shielded" samples and less so in the "unshielded." In the steel samples we see production of a variety of isotopes which will inform our understanding of residual radiation cooldown. Comparison to MARS and DeTra calculations will use this data.

8 Acknowledgments

The contributions from Gary Lauten and the Accelerator Radiation Safety Group are gratefully acknowledged. Access for placement and removal of samples required careful coordination since access demanded that no antiprotons be in the Recycler Ring. We thank the Run Coordinators Cons Gattuso and Mary Convery for their assistance in this coordination.

A Locations for Activation Tag Placement

The locations for this activation study were chosen to match spots where we have carried out a series of residual radiation cool down measurements. One of these was reported in [4]. Photos for that document allow one to identify these locations. Figure 3 shows the location for the "Shielded" activation tags. Figure 4 shows the location for the "Unshielded" activation tags.

References

[1] Bruce C. Brown and Guan Hong Wu. Measuring Correlations Between Beam Loss and Residual Radiation in the Fermilab Main Injector. In Jan Chrin, editor, *Proceedings of the 46th ICFA*

Figure 3: Placement of Geiger Tube for measurement of residual radiation at “Shielded” location on Collimator C307

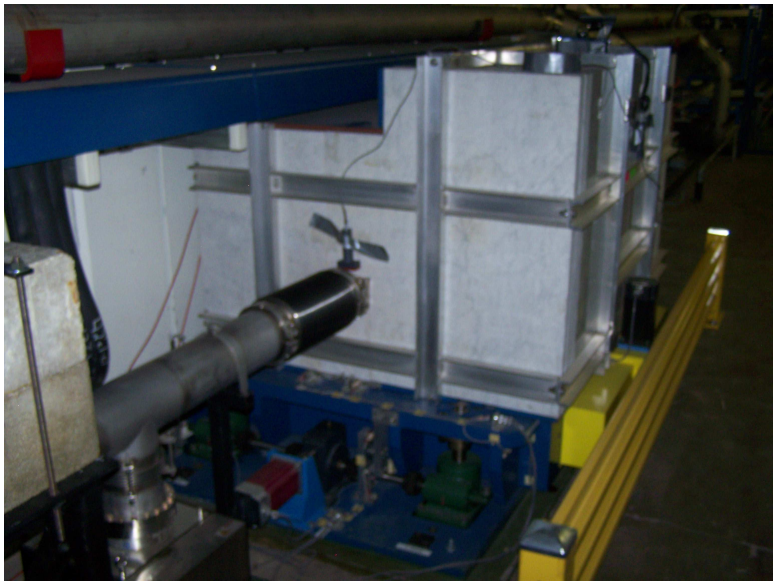

Figure 4: Placement of Geiger Tube for measurement of residual radiation at “Unshielded” location on Collimator C307

Advanced Beam Dynamics Workshop on High-Intensity and High-Brightness Hadron Beams (HB2010), Morschach, Switzerland, 2010. Also available as FERMILAB-CONF-10-368-AD.

[2] Bruce C. Brown. Analysis of Some Crude Main Injector Radiation Cool-down Data. Beams-doc 3219 v1, Fermilab, October 2008.

[3] Bruce C. Brown. Predicting Residual Radiation using Beam Loss Data - Early Results. Beams-doc 3568 v1, Fermilab, March 2010.

[4] Amir Jaehoon Safavi. Comparison of Short Term Cooldown Data for MI Collimator C307 Near Beam and Beside Marble Shielding. Beams-doc 3717 v1, Fermilab, November 2010.

[5] Bruce C. Brown. Main Injector Collimation System Hardware. Beams-doc 2881 v2, Fermilab, April 2008.

[6] A. Baumbaugh, C. Briegel, B. C. Brown, D. Capista, C. Drennan, B. Fellenz, K. Knickerbocker, J. D. Lewis, A. Marchionni, C. Needles, M. Olson, S. Pordes, Z. Shi, D. Still, R. Thurman-Keup, M. Utes, and J. Wu. The upgraded data acquisition system for beam loss monitoring at the Fermilab Tevatron and Main Injector. *JINST*, 6:T11006, 2011. Also available as FERMILAB-PUB-11-618-AD-PPD.

[7] Bruce C. Brown. Analysis Procedures for Al Activation Studies. Beams-doc 3980, Fermilab, November 2011.

[8] Nikolai V. Mokhov. The MARS code system user's guide version 13(95). FN 628, Fermilab, April 1995.

[9] N. V. Mokhov and S. I. Striganov. MARS15 overview. *AIP Conf. Proc.*, 896:50–60, 2007. Also available as FERMILAB-CONF-07-008-AD.

[10] Pertti A. Aarnio. Decay and Transmutation of Nuclides. CMS-NOTE 1998-086, CERN, January 1999.

[11] Marcel Barbier. *Induced Radioactivity*. North-Holland Publishing Company, Amsterdam, London, 1969.

[12] M. Jenko, F. Vodopivec, H. J. Grabke, H. Viefhaus, M. Godec, and D. Steiner Petrovic. Influence of Antimony on the Texture and Properties of 2% Si, 0.3% Al Steel for Non-Oriented Sheet. *Journal de Physique IV*, 5:C7–225, 1995.